Research on Control Strategy of Magnetic Levitation Gravity Compensator Based on Lyapunov Stability Criterion

Research on Control Strategy of Magnetic Levitation Gravity Compensator Based on Lyapunov Stability Criterion

Xiangyu Shi*, Qingqing Mao[a]

State Grid Hubei Electric Power Company Limited Yichang Power Supply Company, Yichang, China

*Corresponding author e-mail: 283801652@foxmail.com, [a]maomay123@163.com

Abstract. A magnetic levitation gravity compensator is designed based on the remanent rewritable characteristics of variable flux permanent magnets. It adopts a coaxial symmetrical structure, which maximizes the use of stray flux and reduces the use of the magnet core, thereby increasing the repulsive density of the device. Through simulation optimization of the design scheme, we extracted the optimal design parameters, so that the repulsion and stiffness displacement characteristics of the working stroke meet the requirements of system self-recovery. At the same time, we have analysed the repulsion and stiffness displacement characteristics of the magnetic levitation gravity compensator. According to Lyapunov stability theory, we designed the dynamic control system of the device and established the workflow of the system. We verified the effectiveness of the design of the device and the reliability of the control system through experiments on the engineering prototype.

1. Introduction

Gravity compensators play an important role in space control mechanisms, multi-spectral isolation devices, high-precision machine tools, and micro-motion tables. At present, the common methods of gravity compensation include pneumatic compensation, mechanical compensation and magnetic levitation compensation. Magnetic levitation compensation has received more and more attention because of its high power density and simple structure [1-6].Earlier, foreign scholars conducted research in this field. In 2004, the ASML Company in the Netherlands first proposed the concept of a magnetic levitation gravity compensator; Hol S carried out prototype design and in-depth theoretical analysis of this type of magnetic suspension gravity compensator [7-8]; The Korea Institute of Science and Technology proposed a flat-type magnetic levitation gravity compensator. The secondary permanent magnet adopts the Halbach structure, and the optimal design of the suspension force and stiffness is achieved by adjusting the height ratio of the permanent magnets [9-10].In recent years, domestic scholars have gradually deepened their research in this field. Yu Li of National University of Defense Technology conducted a detailed theoretical analysis of the magnetic field of hybrid magnetic levitation compensator [11]; Zhang He of Harbin Institute of Technology proposed an axisymmetric magnetic suspension gravity compensator, which designed the zero stiffness working point by using the difference of permanent magnet suction repulsion [12].These studies provide a relatively complete process guidance for the structural design of the magnetic levitation gravity compensator, but the research results are still relatively rare in the control method of the magnetic levitation gravity

compensator. Therefore, based on the study of a magnetic suspension gravity compensator with novel structure, low axial stiffness and compact structure, this paper focuses on the control method of the compensator, and sets the constraints from the perspective of control stability, established a perfect workflow, and finally verified the reliability of this control method through experiments. The control strategy has a certain guiding effect on the design of the magnetic levitation gravity compensator.

2. Magnetic suspension gravity compensator Structure

The structure of the magnetic levitation gravity compensator is shown in Fig1. The load platform is located on the top of the compensator, with a radially magnetized permanent magnet embedded in it, providing axial, meridional support and axial short stroke rapid displacement for gravity loads. Two sets of magnetic levitation force generation systems are placed in the base of the lower part of the compensator: one is a steady-state gravity compensation system using a memory permanent magnet material as an excitation source; the other is an electrically-adjustable gravity compensation system. The two systems share a set of magnetic circuit structures, which reduces the size of the device and increases the power density of the system.

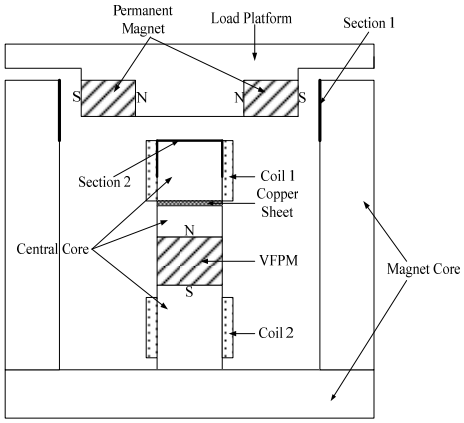

Figure 1. Hybrid excitation magnetic suspension gravity compensator.

The polarization direction of the permanent magnet embedded in the load platform is the same as the polarization direction of the corresponding base core contact surfaces S_1 and S_2 (as shown in Fig. 1), and the magnetic forces are mutually exclusive. We designed the shape of the contact surface to maximize the axial repulsive force of the load platform in equilibrium. The axial magnetic levitation force is mainly provided by the contact surface S_2, and the position of the load platform permanent magnet is higher than the pedestal core contact surface S_2, and the repulsion force thereof has an axial component to compensate the gravity of the load platform. At the same time, when the load platform is biased by horizontal force external disturbance, the repulsion characteristic will also automatically return to the equilibrium position.

The magnetic potential of the susceptor is provided by a series magnetic circuit consisting of a memory permanent magnet and an excitation coil. We will introduce the two as follows. The arrangement of the excitation coil is shown in Figure 1.The magnetic potential of the susceptor is provided by a series magnetic circuit consisting of a memory permanent magnet and an excitation coil. We will introduce the two as follows. The arrangement of the excitation coil is shown in Figure 1. A set of coaxial excitation coils L_1 and L_2 are arranged on the upper and lower half shafts of the center core of the base, and the pulse magnetic field generated by the two coils is shielded by the high conductivity metal sheet in the middle of the central core. They will be closed along their respective magnetic circuits to avoid affecting the total superimposed magnetic field. The conduction of the excitation coils L_1 and L_2 during the load increase and decrease of the load platform is described in detail in the following sections.

3. Mechanical properties of the system

3.1. Gap magnetic field analysis

We simulate the mechanical properties of the magnetic levitation gravity compensator by finite element analysis and virtual displacement method. The two-dimensional structured model was established in Maxwell, and it is shown in fig 2. Here, the axisymmetric model is chosen to simplify the analysis process. Figure 2 shows the magnetic field distribution of the gravity compensator excited only by the memory permanent magnet. It can be seen from the figure that the magnetic lines on the left and right sides of the load platform and the magnetic lines in the adjacent core mutually repel each other, and the main force of the interaction force is upward. Since the magnetic flux density in the horizontal direction of the right side is larger than the magnetic flux density in the horizontal direction of the left side, the force on the horizontal side of the load platform is unbalanced. We consider that the gravity compensator is designed as a ring-shaped symmetrical structure, and the unbalance forces on both sides cancel each other out, and the total horizontal force is 0. The magnetic compensator is not provided with a magnetically permeable structure at the top, the magnetic flux is relatively dispersed, and the load permanent magnet is loaded with a clockwise rotational moment. However, since we adopt a ring-shaped symmetrical structure, the clockwise rotational moments are superimposed on each other and the upward suction force is present as a whole, so this design increases the repulsive density of the device.

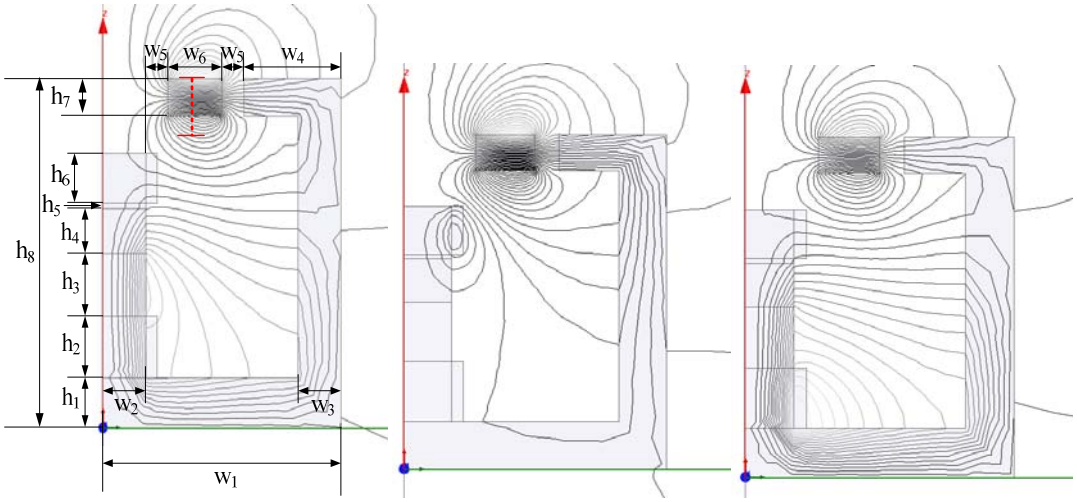

Figure 2. Distribution of magnetic field.

Picture in the middle shows the magnetic field distribution when the exciting coil L_1 acts on the steady state current alone. Because the relative magnetic permeability of the central memory permanent magnet is low, the magnetic field lines are mainly closed by the air gap and the outer core. Therefore, the function of providing the required repulsive force to the load platform without affecting the demagnetization of the central memory permanent magnet of the pedestal is realized. The last picture is a magnetic field distribution under the action of the steady-state current of the memory permanent magnet and the exciting coil L_2. Compared with the magnetic field distribution in the left, in addition to the increase in the air gap flux density near the exciting coil L_2, the main difference between the two is that the superposition of the two excitation sources increases the magnetic flux density in the core, and the magnetic force generated by the permanent magnets of the load platform is shifted, that is, the repulsive force of the device is improved. The operating conditions shown in the figure are the process by which the gravity compensator tracks the load boost by applying an exciting current after the load is increased.

3.2. Repulsive force-displacement characteristics analysis

The gravity compensator is applied to a special field, and the working stroke is short, and the movable range is 2mm above and below the balance position. In order to ensure the self-recovery characteristics of the equilibrium position, the ideal axial repulsion characteristic curve in the working stroke should show a monotonous increasing trend. The load platform is disturbed by axial external forces, shifting up or down, that is, the repulsive force of the new position should move the platform to the equilibrium point. In addition, the axial repulsion stiffness should have a zero point in the equilibrium position, and the ideal characteristic curve is preferably a tan function of the zero crossing point. Figure 3 shows the distribution of axial repulsive force and axial stiffness of the load platform from the top end along the distance from the top core horizontal plane to the downward offset of 8 mm (shown in red dotted line in figure 3 when the memory permanent magnet is separately excited. According to the engineering requirements, the interval Z_l [-2*mm*, 2*mm*] marked in figure 2 is selected as the working stroke of the device.

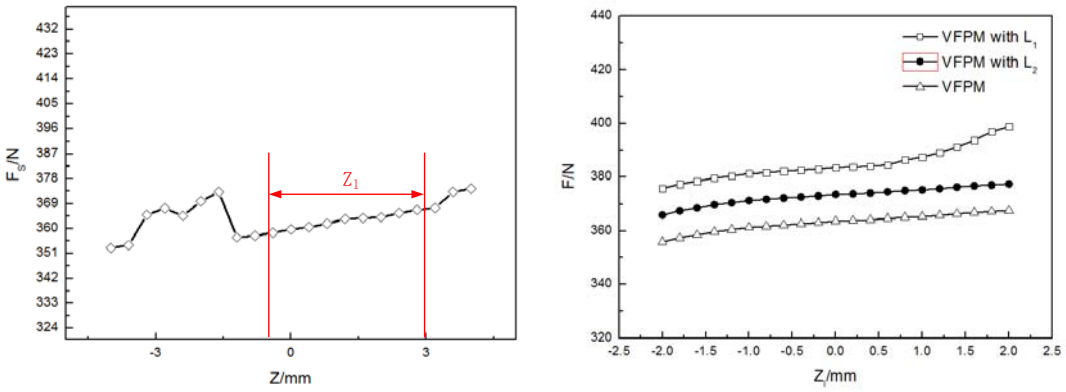

Figure 3. Effective working stroke of memory permanent magnet.

The picture in the right is a comparison diagram of the repulsion-displacement characteristics when the memory permanent magnet acts alone, the memory permanent magnet and the exciting coil L_1 act together, and the memory permanent magnet and the exciting coil L_2 act together. Since the magnetic flux path of the memory permanent magnet and the magnetic flux path of the exciting coil L_2 are the same, the performance of the displacement characteristics of the individual levitation force-displacement characteristics and the superimposed levitation force are also very similar. The magnetic flux density generated by the excitation coil L_1 monotonically increases on the working stroke, and the superimposed repulsion-displacement characteristic curve appears as an oblique bowl type, and the zero stiffness point is shifted to some extent. However, this kind of working condition only occurs in the early stage of the process of reducing the residual magnetism of the memory permanent magnet and has a short duration, which has little influence on the stability of the system.

4. Design of control system

4.1. Gravity compensator control system model

The gravity compensator control system uses the way of changing the flow state of the two sets of excitation coils to track the load on the load platform. The total mass of the load and the platform is m, the total gravity is mg, the axial repulsive force provided by the memory permanent magnet is F_{jy}, and the axial repulsive forces provided by the two excitation coils are F_{l1} and F_{l2}, respectively. The device has three working modes:

1. When the platform is stable:

$$F_{jy} = mg \tag{1}$$

F_{jy} is proportional to the residual magnet Br of the memory permanent magnet, and the residual magnet Br can be erased by the exciting coil L_2, which is proportional to the pulse current i_2 of the exciting coil L_2.We use the polynomial to fit the relationship between pulse current and F_{jy} according to the magnetization characteristic curve of the memory permanent magnet used:

$$F_{jy}(i) = a_1 i_2^2 + b_1 i_2 + c_1 \tag{2}$$

In the middle, the rush current i_2 is provided by a voltage source:

$$\dot{i}_2 = \frac{u}{L_2} \tag{3}$$

2. When the platform load is reduced:

$$mg - F_{jy} - F_{I1} = ma \tag{4}$$

The a in the equation is the dynamic acceleration of the load platform. At this time, the exciting coil L_2 is demagnetized by the pulse current, and is shielded by the metal piece in the middle of the center core, and the pulsed magnetic field does not affect the axial repulsion of the load platform. The exciting coil L_1 passes the dynamic current i1 to compensate the difference between the demagnetization point of the memory permanent magnet and the residual magnetic point.

3. When the platform load is increased, the excitation coil L_2 is magnetized by the pulse current. If the load is greater than the maximum axial repulsive force that the memory permanent magnet can provide, the excitation coil L_2 needs to provide an additional stable axis repulsive force. The exciting coil L_1 compensates for the difference between the highest magnetic flux density point of the memory permanent magnet and the residual magnetic point by the dynamic current i_1:

$$mg - F_{jy} - F_{I1} - F_{I2} = ma \tag{5}$$

Since modes 1 and 3 can be extrapolated with modal 2, here we focus on the control characteristics of the device when it is in modal 2. The time at which the load on the load platform suddenly increases is t_0, the time constant of the exciting coil is τ, and the axial repulsion reaches a maximum value after 3τ, and then stops moving at the time t1 under the action of the constant deceleration a. The total moving distance S is:

$$S = \{\int_{t_0}^{3\tau} [(mg - F_{jy} - F_{I1})\, t/m]dt + \int_{t_1}^{3\tau} at \cdot dt\} \leq 2 \tag{6}$$

Bringing the formula (3) into the formula (2), in order to simplify the analysis, the resultant force of F_{jy} and F_{I1} is fitted to the equation (6) by the same polynomial fitting, and finally the control model of the system is obtained:

$$F_Z(i, S) = A \cdot S + Bi^2 + Ci \tag{7}$$

$$\dot{S} = \mathrm{v} \tag{8}$$

$$\dot{v} = g - F_Z(i, S)/m \tag{9}$$

4.2. Analysis of control characteristics based on lyapunov theory

According to formula (7), the controlled part of the gravity compensator is a nonlinear system. Here, the Lyapunov stability theory (direct method) suitable for nonlinear and time-varying systems is selected to analyse the control characteristics of the device [16].

Further simplify equation (9), ignoring high-order terms:

$$\dot{e}_s + \dot{S}_0 = e_v + \mathrm{v}_0 \tag{10}$$

$$\begin{aligned} \dot{e}_v + \dot{v}_0 = {} & g - Ae_s/m \\ & -AS_0/m - Ci/m \end{aligned} \tag{11}$$

According to formula (11) :

$$\begin{aligned} i = {} & mg/C - Ae_s/C \\ & -AS_0/C - m(\dot{e}_v + \dot{v}_0)/C \end{aligned} \tag{12}$$

The control signals are synthesized from the error dynamics model of the system to obtain the desired closed-loop function u consists of two parts [17], one is the real-time value u obtained according to equation (9), and the other is C obtained from the error dynamics model of the system. The stability of the system error dynamics model can be proved by the following equation:

Set the function:

$$V(x) = 1/(2\mathrm{m}\, e_v^2) + mgS \tag{13}$$

$$\dot{V}(x) = me_v \dot{e}_v + mg \dot{e}_s \tag{14}$$

Substituting them into equation (14) gives:

$$\dot{V}(x) = me_v(2g - Ae_s/m - Ci/m) \tag{15}$$

Because we can design the control parameter C so that the equation (15) is always negative in the domain, thus demonstrating that the control system is globally asymptotically stable at the equilibrium point.

5. Experimental verification

In order to verify the reliability of the magnetic levitation gravity compensator and its control system proposed in this paper, we have developed an experimental prototype and built a test platform. The location of the dimension parameters is shown in Figure 4. The memory permanent magnet adopts the axial magnetic cylinder with permanent magnetic material grade LNGT72, and the permanent magnet magnetic ring of the load platform is made of sintered NdFeB magnet. with permanent magnetic material grade LNGT72, and the permanent magnet magnetic ring of the load platform is made of sintered NdFeB magnet. We use the BM24R type load cell of AVIC to measure the load, and use the grating ruler to measure the displacement of the load platform. The above measurement results are displayed on the host computer in real time through the data acquisition card.

Figure 4 shows the repulsion-displacement characteristic curve of the individual excitation of the memory permanent magnet measured by simulation and experiment. Comparing with the simulation results, we found that the actual measured repulsive force was low overall, and the average deviation rate was 6%. We think that the cause of this deviation may be that the magnetic fields generated by the two permanent magnets cancel each other out, causing the working point of the memory permanent magnet to shift on the hysteresis curve. In addition, because the two curves did not change significantly except the amplitude, indicating that the stiffness-displacement characteristics approached, the zero-stiffness point did not shift significantly.

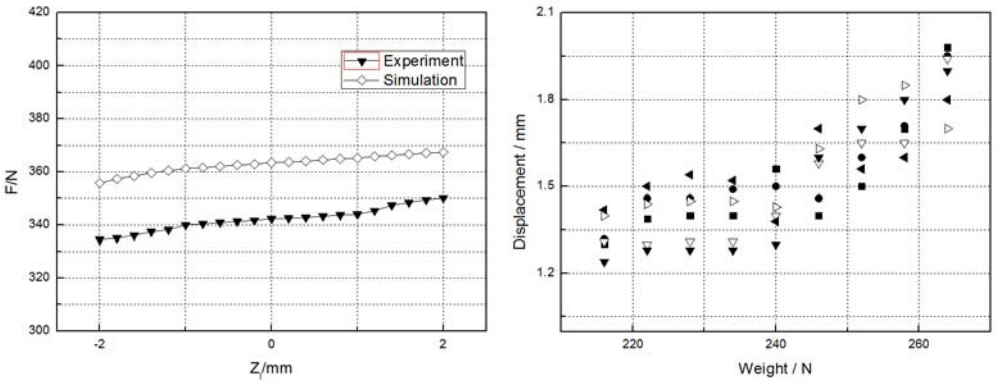

Figure 4. Measured and simulated repulsive force - displacement characteristic curve.

The load-offset characteristics at load disturbance are shown in the right. This figure shows the dynamic response of the control system to the abrupt load. This figure shows the dynamic response of the control system to the abrupt load. The horizontal axis indicates the magnitude of the applied load. The memory is residued to provide 70% of the repulsive force as the center point, and the load is increased or decreased by 10% as the effective control interval. The vertical axis represents the distance traveled by the load platform when the disturbance speed returns to the first zero point under the control system. A total of six sets of data were recorded at each sampling point to verify the stability of the control system. As can be seen from the figure, in the effective control interval, the offset point can be controlled within 2mm. However, the offset distance required to increase the load is greater than the offset when the load is reduced. And with the increase of the absolute value of the load, the nonlinearity of the offset increases. The preliminary analysis shows that the magnetic flux density of the memory permanent magnet approaches the saturation point. Therefore, the thickness of the memory permanent magnet can be appropriately increased in engineering applications to meet the requirements of the control interval.

6. Conclusion

We designed a magnetic levitation gravity compensator based on the characteristics of memory permanent magnet rewritable remanence. It adopts a coaxial symmetrical structure, which maximizes

the use of stray magnetic flux density and reduces the use of the core, thereby increasing the repulsive density of the device. Then we optimized the design parameters and extracted the best design parameters.

The axial repulsive characteristic curve of the memory permanent magnet during single excitation is monotonically increasing, and the axial repulsive characteristic curve of the excitation coil and the memory permanent magnet is presented as a slanting bowl type. The zero stiffness point displacement in different modes meets the engineering requirements.

We analyzed the characteristics of the repulsion and stiffness displacement of the magnetic levitation gravity compensator. Based on Lyapunov stability theory, the dynamic control system of the device is designed and the workflow of the system is established. The design of the device is verified by experiments on the engineering prototype. In the effective control interval, the offset point can be controlled within a range of 2 *mm*, but the offset distance required to increase the load is greater than the offset when the load is reduced. And with the increase of the absolute value of the load, the degree of nonlinearity of the offset increases.

Acknowledgments
This work was financially supported by SGCC Innovation plan.

References

[1] Post R F, Ryutor D D. The inductrack: a simpler approach to magnetic levitation [J]. IEEE Transactions on Applied Superconductivity, 2000, 10(1): 901-904.
[2] Bergh V D, Hugo H, Kratz, et al. Magnetic levitation and propulsion system: US, Patent Number 6827022 [P]. 2004-12-07.
[3] Verma S, Kim W J, Gu J. Six-axis nanopositioning device with precision magnetic levitation technology[J]. IEEE/ASME Transactions on Mechatronics, 2004, 9(2): 384-391.
[4] Verma S, Kim W J, Shakir H. Multi-axis maglev nanopositioner for precision manufacturing and manipulation applications [J]. IEEE Transactions on Industry Applications, 2005, 41(5): 1159-1167.
[5] Verma S, Shakir H, Kim W J. Novel electromagnetic actuation scheme for multiaxis nanopositioning[J]. IEEE Transactions on Magnetics, 2006, 42 (8): 2052- 2062.
[6] Gajdusek M, Damen A, van den Bosch P. Identification and parameter-varying decoupling of a 3-DOF platform with manipulator [C]. International Symposium on Power Electronics, Electrical Drives, Automation and Motion, Ischia, Italy, 2008: 691-696.
[7] Hol S, Buis E, Weerdt R. Lithographic apparatus, magnetic support for use therein, device manufac-turing method, and device manufactured thereby: US, 6831285B2 [P].
[8] Hol S, Lomonova E, Vandenput A. Design of a magnetic gravity compensation system [J]. Precision Engineering, 2006, 30 (3): 265-273.
[9] Choi Y M, Lee M G, Gweon D G, et al. A new magnetic bearing using halbach magnet arrays for a magnetic levitation stage [J]. Review of Scientific Instruments, 2009, 80(4): 045106(1-9).
[10] Choi Y M, Gweon D G. A high-precision dual-servo stage using halbach linear active magnetic bearings [J]. IEEE/ASME Transactions on Mechatronic, 2011, 16(5): 925-931.
[11] Yu Li, Zhang Zhuoran, Chen Zhihui, et al. Analysis and verification of the doubly salient brushless dc generators for automobile auxiliary power unit application [J]. IEEE Transactions on Industrial Electronics, 2014, 61 (12): 6655-6663.
[12] Zhang He, Kou Baoquan, Jin YinXi, Zhang Hailin. A Cylindrical Magnetic Levitation Gravity Compensator with Halbach Secondary Structure [J]. Transactions of China Electrotechnical Society, 2016, 31(6): 30-37.
[13] Jang Y J, Lee J H, Kim J C. Permanent magnet dema-gnetization characteristics analysis of a variable flux memory motor using coupled preisach modeling and FEM [C]. IEEE International Magnetics Conference, Digest Record of Conference, 2005: 735-736.

[14] Lim H B, Kim Y H, Lee M M. Permanent magnet demagnetization characteristics analysis of a variable flux memory motor using coupled preisach modeling and FEM [C]. IEEE Electric Machines and Drives Conference, 2007, 1: 647-651.
[15] Chen Yiguang, Pan Wei, Shen Yonghuan, et al. Magnetic field analysis of interior composite-rotor controllable-flux permanent magnet synchronous machine [J]. Transactions of Tianjin University, 2006, 12 (5): 330-334.
[16] Rahmani S, Hamadi A, AI-Haddad K. A lyapunov function based control for a three phase shunt hybrid active filter [J]. IEEE Transactions on Industrial Electronics, 2012, 59 (3): 1418-1429.
[17] Li Lanfang, Yang Honggeng, Guo Weiming, et al. Lyapunov-based current stability control method of active power filter [J]. Transactions of China Electrotechnical Society, 2012, 27(9): 78-86.